群流星出現率の周期的変動について.

1980・9・28　武蔵高 O・B　大西 洋

○ この報告は、昭和46年度に武蔵高校太陽観測部が発表した、同名の論文に基づいています。

○ ランダム現象の待ち時間(t)　／待ち時間がこれより長くなる確率

ランダムである ⇒ $P_{t>T}(t>T+S) = P(t>S)$ …①

一般に $P_A(B)\cdot P(A) = P(A\cap B)$, 特に $A\supseteq B$ のとき $P(A\cap B) = P(B)$

$\therefore P(t>S)\cdot P(t>T) = P(t>T+S)$　($\because$ $t>T+S>T$)

ここで, $1\geq f(T) = P(t>T)\geq 0$ とおく.

$f(S)\cdot f(T) = f(S+T)$

Sで微分. $f(T)\cdot f'(S) = f'(S+T)$

$S=0$　$f'(0)\cdot f(T) = f'(T)$

Tで積分　$f(t) = e^{-\lambda t}$

$f(0)$ の max は $T=0$ のとき

$f(0)=1$. 明らかに $f'(0)\leq 0$

ゆえに, $f'(0) = -\lambda$ $(\lambda\geq 0)$ とおく.

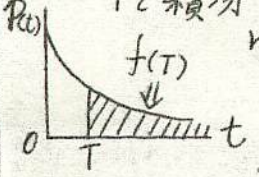

ゆえに. tの確率分布 $P(t) = (1-f(t))' = \lambda e^{-\lambda t}$

ここで $\int_0^\infty t\cdot(P(t))\,dt = \frac{1}{\lambda}$; tの期待値

つまり. λは単位時間あたりの出現数 (出現率)

○観測結果 (1961～64・66・71・78)

さて，前節で出現率が矩形周期変動をする場合の到着分布を調べた際に，その到着分布にできるピークは周期より若干小さな所にできる事が判明した。このことから，実際の流星群の流星出現率が第７表の様な周期で変動していれば，実際の到着分布にできているピークの位置と各々の周期との間に単純な関係がある筈である。第７表と第７図を比較すると各周期は以下の様に到着分布のピークとして単純な位置関係が成り立っている。

61年　／右ヘリジ・グラフから求めた周期

70 sec	→	55～65	
90	→	85	(η周期)
130	→	～120～	(φ周期)

62年

55(110) sec	→	45	(μ周期)
70	→	65	
90	→	85	(η周期)

64年 8/9

50 sec	→	45	(μ周期)
80	→	65～75	
120	→	115	(φ周期)

64年 8/10

55(110) sec	→	45	(μ周期)

66年

60 sec	→	50, 105?	(μ周期)
150			

○周期的変動の成因

1) 流星群が形成される時.
2) 地球大気に突入するとき.
3) 太陽系内を運動するとき.
4) 流星観測時.

第7図　ペルセウス座流星群の到着分布

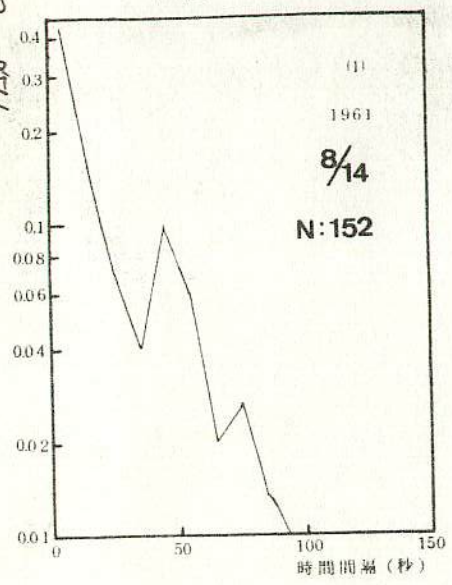

(1)
1961
8/14
N:152

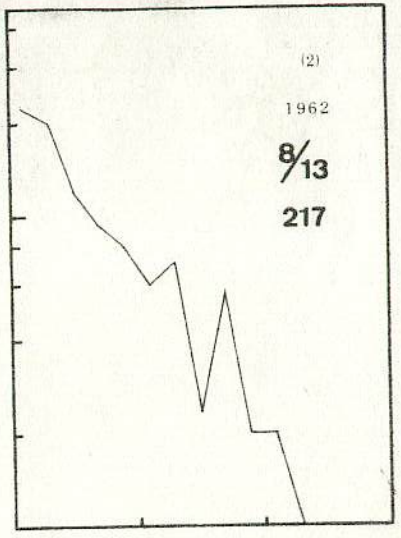

(2)
1962
8/13
217

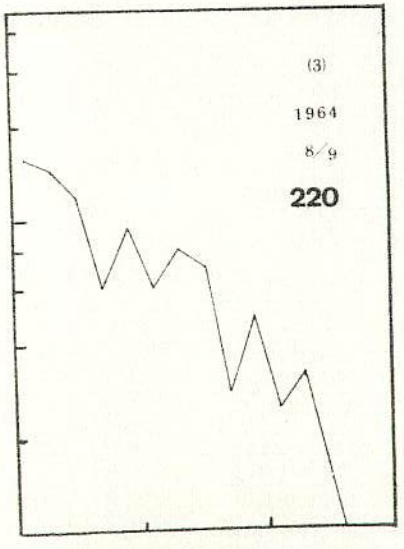

(3)
1964
8/9
220

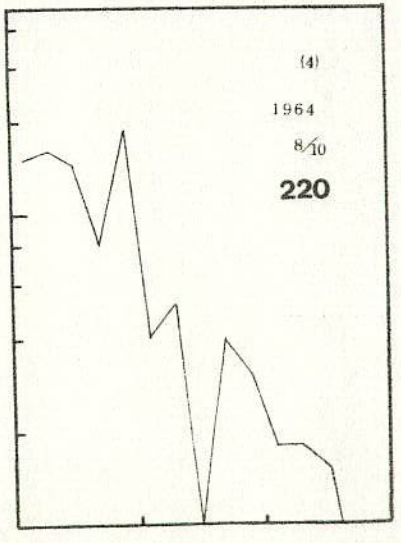

(4)
1964
8/10
220

第7図　（つづき）

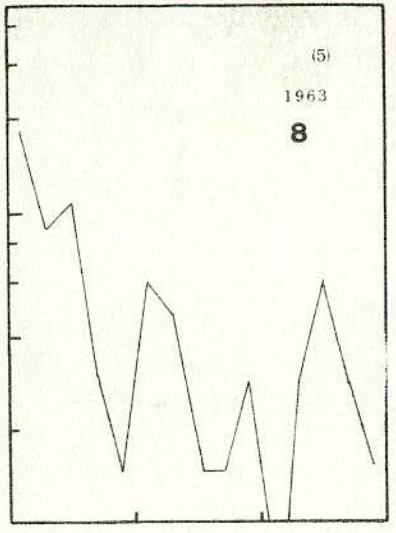

(5)
1963
8

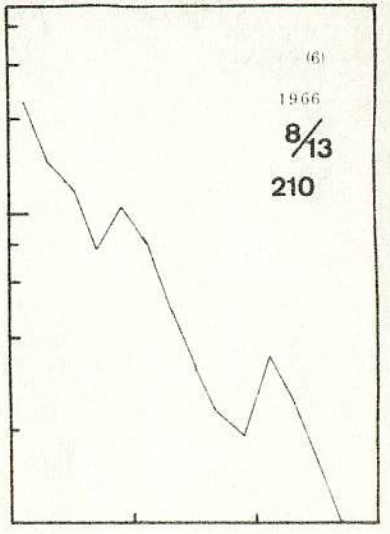

(6)
1966
8/13
210

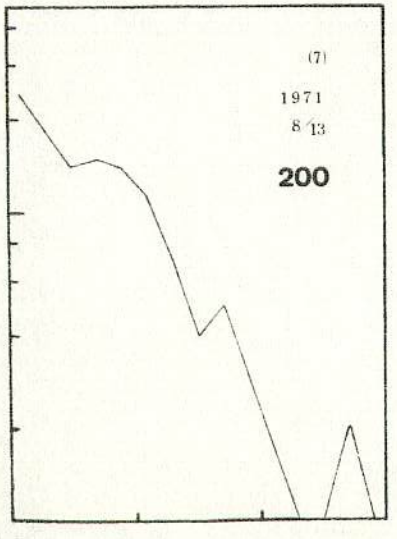

(7)
1971
8/13
200

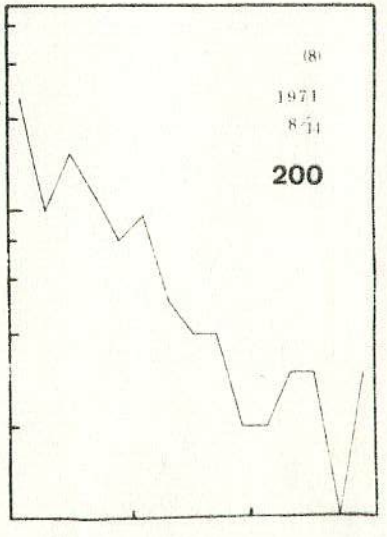

(8)
1971
8/11
200

MSS-011
11th MSS

本人は来なかった。

「流星の出現間隔について」

群馬星の会

須永　勲

〒376　桐生市川内町5丁目2932
TEL.　0277 65 8606

第21回流星会議

MSS-011

流星を観測すると、時には、たてつづけに流れ、また ある時には1つも 流れないことが よくある。これは、いわゆる 流星の『豆まき現象』とよばれるもので、流星の出現間隔に ムラが あることを示している。

今回は、本当に この 豆まき現象は 存在するのか、また流星が、ランダムに出現すると仮定した時の 出現間隔は どのような分布を するのかを考え、流星が ランダムに 出現しているか どうかと考察する

＊　　＊

まず最初に 流星が ランダムに出現した時の出現間隔（いま これを理論的出現間隔とよぶ）の分布を考える。そのため、乱数を使って ランダムに 流れる仮想流星を、次のようにしてつくる。

1. 0と1の区間に、なるべく 多くの一様乱数を発生させ、小さいものから並べる。この時 乱数1個 1個が 流星の出現時刻である。

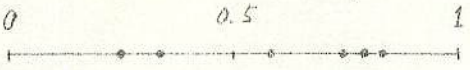

2. 次に 0, 1区間を観測時間と考え、

（乱数の間隔）×（観測時間）

を計算し、実際の観測時間とマッチするようにする。

3. 2. の乱数の間隔 C^* を求める。ただし、この場合、乱数の個数が多いと当然 その乱数の間隔が短かくなってしまう。そこで、実際に流れた流星の個数を考慮し、これと同じ条件にするため、発生させた乱数の個数を n'、実際に流れた流星の個数を n とすると、全くランダムに流星が流れると仮定した時の出現間隔（理論的出現間隔）C は

$$C = C^* \cdot \frac{n'}{n}$$

となる。例えば、実際の流星の2倍の個数の乱数を発生させた

なら、その乱数の間隔の平均値は、実際の流星の出現間隔の平均値の 1/2 になってしまうので、乱数の間隔を 2倍にし、実際の流星の平均的出現間隔に合わせる。

4. こうして得られた出現間隔を、いくつかの区間に分け、それに属する現間隔の個数を求め、実際の流星の出現間隔と比較する。
（当然、発生させた乱数の個数を実際の流星数に合わせる）

以上のようにして、流星がランダムに出現した時の理論的出現間隔を得たが、いま、この分布と、実際の流星の出現間隔の分布をくらべると、Fig. 1 ～ Fig. 4 のようなグラフになる。

この図をみてもわかるとおり、

1° ほぼ実際の流星の出現間隔と、その理論値には、概形的には同じである。

2° 流星がランダムに流れるとした時の理論値は、当初予想していた出現間隔の平均値が多い山型の分布にはならず、出現間隔の短かい流星が多く、またすそのの広い分布となっている。

ということがわかる。以上のことより、流星の〝まめまき現象〟は、ある程度、ランダム出現から予想されることなのである。とは言え、やはり、群流星、散在流星とも、出現間隔が短かいところでは、理論値より、実際の流星の個数の方が、すべてにわたって上回っており、特に群流星の場合には著しく、'79 Q1 などは、理論値の 1.3倍以上になっていて、かなりの食い違いが見られ、流星の突発性を裏付けている。

また、出現間隔が、相当長

Table 1 ～ Table 4 の説明

＊ 86.747 ＊ …… 出現間隔の平均値

OBSERVED …… 観測値 O

COMPUTED …… 理論値 C

(O−C)2/E …… $(O-C)^2/C$

MSS-011

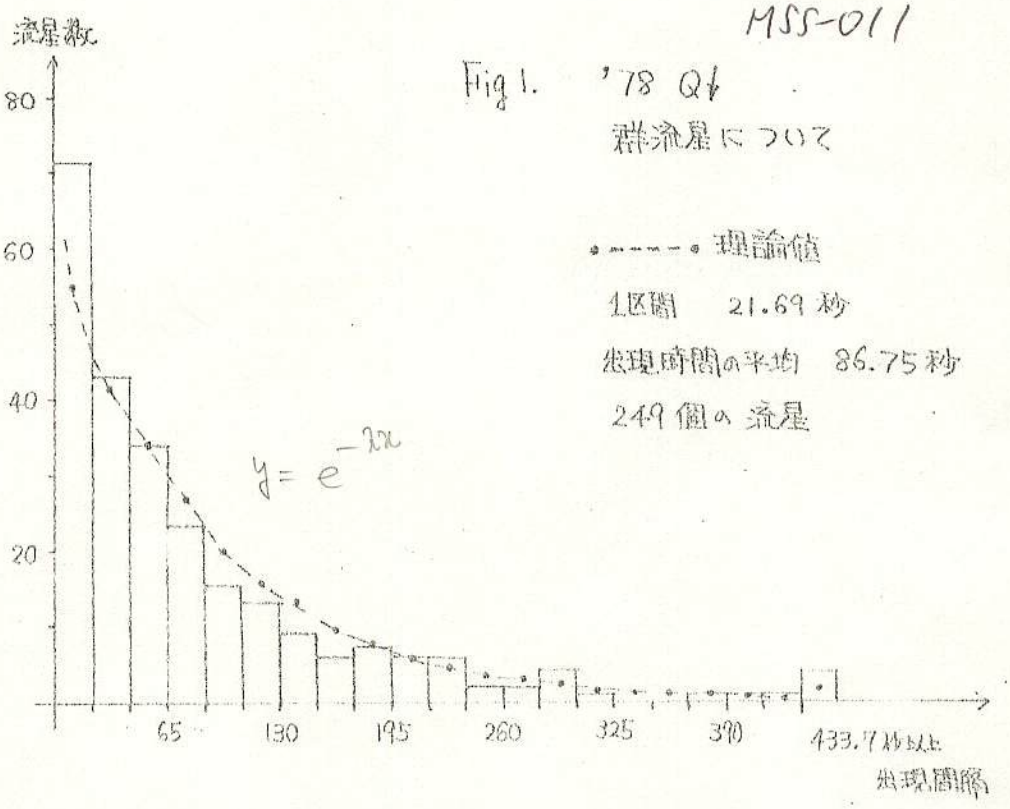

Fig 1. '78 Q4
群流星について

•-----• 理論値
1区間 21.69秒
出現時間の平均 86.75秒
249個の流星

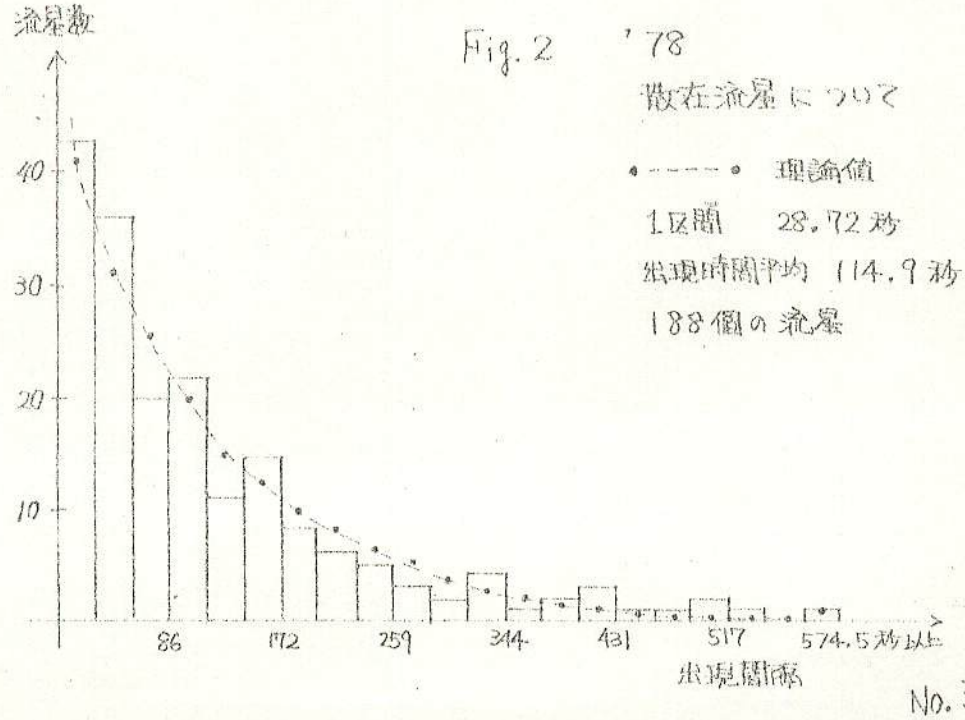

Fig. 2 '78
散在流星について

•-----• 理論値
1区間 28.72秒
出現時間平均 114.9秒
188個の流星

M55-011

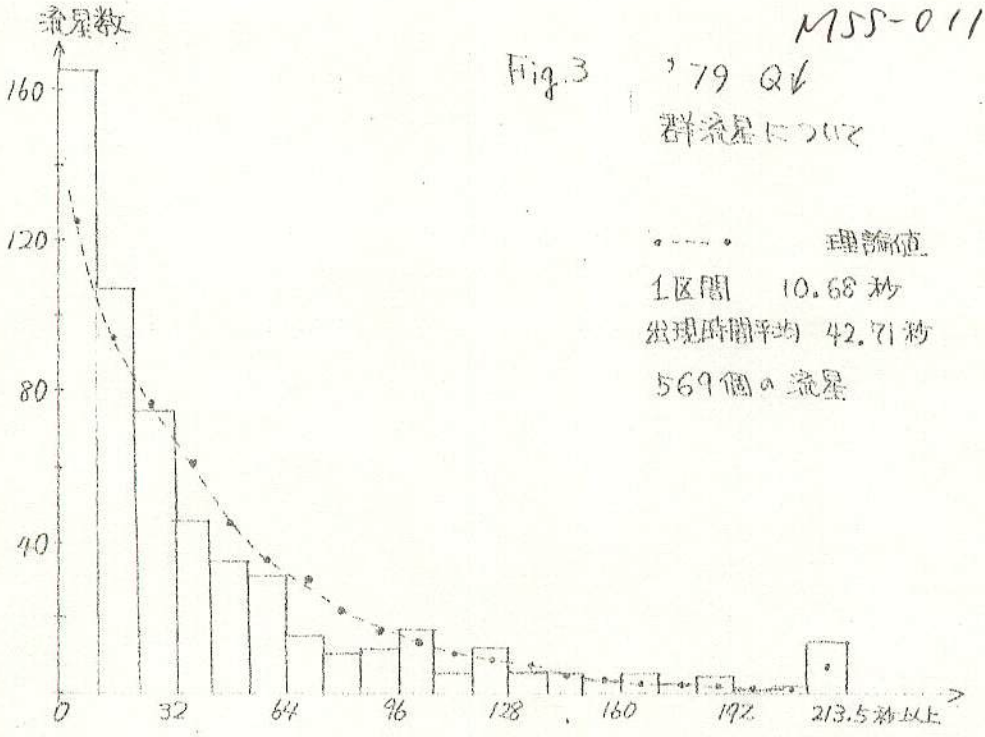

Fig.3 '79 Qr
群流星について

・---・ 理論値
1区間 10.68秒
出現時間平均 42.71秒
569個の流星

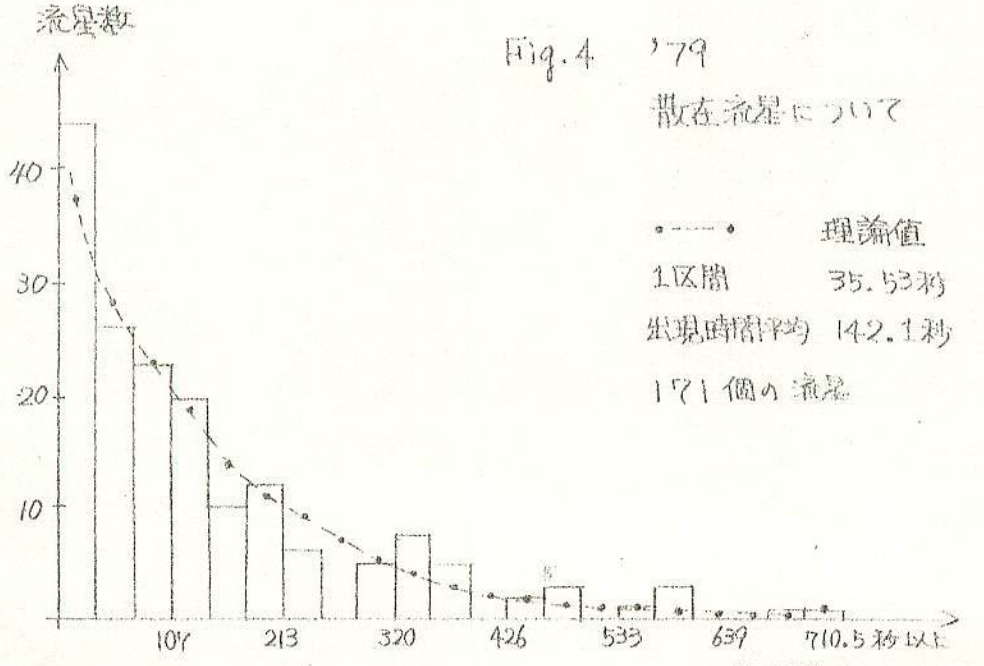

Fig.4 '79
散在流星について

・---・ 理論値
1区間 35.53秒
出現時間平均 142.1秒
171個の流星

MSS-011

Table 1 '78 Q1 群流星

* 86.747 **

KUKAN	OBSERVED	COMPUTED	(O-C)**2/E
0.0 - 21.69	71	55.0	257.1
21.69- 43.37	43	41.6	1.9
43.37- 65.06	34	34.0	0.0
65.06- 86.75	23	26.7	13.4
86.75- 108.43	15	19.8	23.4
108.43- 130.12	13	15.6	6.6
130.12- 151.81	9	13.1	17.1
151.81- 173.49	6	9.5	12.6
173.49- 195.18	7	7.9	0.1
195.18- 216.87	6	5.8	0.0
216.87- 238.55	6	4.4	2.5
238.55- 260.24	2	3.9	3.5
260.24- 281.93	2	3.0	1.0
281.93- 303.61	4	2.0	4.1
303.61- 325.30	1	1.8	0.6
325.30- 346.99	0	1.2	1.4
346.99- 368.67	0	1.0	1.0
368.67- 390.36	1	0.8	0.1
390.36- 412.05	0	0.6	0.4
412.05- 433.73	1	0.3	0.5
433.73-	4	1.5	6.2

KOSU= 249 (O-C)2/I GOKEI = 22.407

No.5

Table 2 '78 散在流星 MSS-011

* 114.894 *

KUKAN	OBSERVED	COMPUTED	(O-C)2/E
0.0 - 28.72	43	41.5	0.054
28.72- 57.45	36	31.4	0.670
57.45- 86.17	20	25.7	1.262
86.17- 114.89	22	20.1	0.173
114.89- 143.62	11	15.0	1.056
143.62- 172.34	14	11.8	0.431
172.34- 201.06	8	9.9	0.371
201.06- 229.79	6	7.2	0.202
229.79- 258.51	5	5.6	0.060
258.51- 287.23	3	4.4	0.447
287.23- 315.96	2	3.3	0.536
315.96- 344.68	4	2.9	0.391
344.68- 373.40	1	2.3	0.712
373.40- 402.13	2	1.5	0.176
402.13- 430.85	3	1.3	2.090
430.85- 459.57	1	0.9	0.009
459.57- 488.30	1	0.8	0.070
488.30- 517.02	2	0.6	3.480
517.02- 545.74	1	0.5	0.655
545.74- 574.47	0	0.2	0.219
574.47-	1	1.1	0.018

KOSU= 188 (O-C)2/F GOKEI = 13.082

No.6

MSS-011

Table 3 '79 Q1 群流星

* 42.707 *

KUKAN	OBSERVED	COMPUTED	(O-C)2/E
0.0 - 10.68	165	125.6	12.355
10.68- 21.35	107	95.1	1.497
21.35- 32.03	74	77.7	0.173
32.03- 42.71	46	60.9	3.638
42.71- 53.38	35	45.3	2.335
53.38- 64.06	31	35.6	0.597
64.06- 74.74	15	30.1	7.547
74.74- 85.41	10	21.8	6.396
85.41- 96.09	11	16.9	2.076
96.09- 106.77	16	13.3	0.537
106.77- 117.44	5	10.1	2.575
117.44- 128.12	11	8.9	0.513
128.12- 138.80	5	6.9	0.512
138.80- 149.47	5	4.5	0.054
149.47- 160.15	3	4.0	0.263
160.15- 170.83	5	2.8	1.841
170.83- 181.50	2	2.3	0.045
181.50- 192.18	4	1.8	2.874
192.18- 202.86	1	1.4	0.102
202.86- 213.53	2	0.7	2.689
213.53-	13	3.5	25.673

KOSU= 569 (O-C)2/E GOKEI = 74.293

MSS-011

Table 4 '79 散在流星

* 142.105 *

KUKAN	OBSERVED	COMPUTED	(O-C)2/E
0.0 - 35.53	44	37.7	1.035
35.53- 71.05	26	28.6	0.231
71.05- 106.58	23	23.3	0.005
106.58- 142.11	20	18.3	0.159
142.11- 177.63	10	13.6	0.957
177.63- 213.16	13	10.7	0.494
213.16- 248.68	6	9.0	1.019
248.68- 284.21	0	6.6	6.555
284.21- 319.74	5	5.1	0.001
319.74- 355.26	7	4.0	2.241
355.26- 390.79	5	3.0	1.272
390.79- 426.32	0	2.7	2.665
426.32- 461.84	2	2.1	0.002
461.84- 497.37	3	1.4	2.002
497.37- 532.89	0	1.2	1.211
532.89- 568.42	1	0.8	0.036
568.42- 603.95	3	0.7	7.588
603.95- 639.47	0	0.5	0.527
639.47- 675.00	0	0.4	0.413
675.00- 710.53	1	0.2	3.212
710.53-	1	1.1	0.003

KOSU= 171 (O-C)2/E GOKEI = 31.629

No.8

いものが、実際に数多く存在している。 MSS-011

*　　*

次に、今回観測された流星が、ランダム出現であるかどうかを検定する。観測値が理論値によくあてはまっていれば、ランダム出現していると考え、そうでなければ、ランダム出現ではないと考える。検定方法としては、χ^2 適合度検定を用いる。

ある出現間隔の区間に実際に流星数を O、ランダムに流れると仮定した時の理論値（期待値）を C とする時、$(O-C)^2/C$ をすべての出現区間にわたって計算し、その和

$$\chi^2 = \sum \frac{(O-C)^2}{C}$$

を求める。O-C が大きければ、当然 χ^2 は大きくなり、ランダム出現とは言いがたくなる。今回の場合、危険率 5% で検定すると、Table 5 のようになる。

Table 5　.ランダム性の検定

	区間の分割数	χ^2	危険率 5% の臨界値	ランダム性
'78 群流星	41	42.83	55.8	○
	21	22.41	31.4	○
	11	13.48	18.31	○
	6	9.49	11.07	○
'78 散在流星	41	48.01	55.8	○
	21	13.08	31.4	○
	11	5.65	18.31	○
	6	3.01	11.07	○
'79 群流星	41	127.10	55.8	×
	21	74.29	31.4	×
	11	59.32	18.31	×
	6	43.95	11.07	×
'79 散在流星	41	54.01	55.8	○
	21	31.63	31.4	○
	11	11.31	18.31	○
	6	6.14	11.07	○

MSS-011

ここで、Table 5 の分割数とは、区間をいくつに分けたかということで、区間分割数による流星の理論値と観測値のちがいも考慮してみた。Table 5 を見てもわかるとおり、'79 Q♯ 以外はすべて 5% の危険率はあるが〝実際の流星はランダム出現している〟ということができる。'79 Q♯ の場合は、流星の出現が明け方に集中したため、流星出現の少ない頃は、出現間隔が比較的長いところに分類され、流星出現の多い時は、出現間隔の比較的短いところに分類されてしまったためだと思われる。したがって、流星はほぼランダムに出現していることがわかる。さらに、散在流星の方が群流星より、χ^2 が小さく、よりランダムに流れていると思われる。

＊　　＊

以上より、〝流星のまめまき現象は、流星出現のランダム性から、ある程度予想され、また、群流星、散在流星とも、ほとんどランダムに出現している〟という結果になった。しかし、問題点として、群流星は R.P の高度、時刻により当然出現数がちがってくるので、$23^h \sim 6^h$ などという長い観測時間のデータを一緒に扱うのはどうかというのが考えられる。散在流星についても、日変化（朝方流星が多い）があるので、同様である。また、群流星は、Q♯ のみの観測であるので、すべての流星群が、そうであるとは言いがたい。さらに、散在流星は、Q♯ 観測中に出現したものであるということも考慮しなければならない。

＊　　＊

備考　・使用した computer

群馬大工学部 FACOM 230 38

・流星のデータ

1978 Q♯

日時：1月3日 23^h ～ 4日 5^h

観測地：群馬県勢多郡粕川

方法：6人によるグループカウント

観測者：KESA（本校高校地学部 & 旧OB会）

1979 Q♯

日時：1月3日 23^h15^m ～ 4日 6^h

観測地：群馬県勢多郡粕川

方法：4人によるグループカウント

観測者：KESA

1980 年 8 月 27

流星の待ち時間による出現数の確率的考察

高宮学園　淡路俊雄

1. 昔の流星物理セミナーに、おいて重野氏や大西氏が発表された待ち時間（豆まき現象）の研究を、逆にしたものだと考えてください。

前提条件　流星の出現は乱雑である。

一般に待ち時間の出現確率は、

$$f(t)=ae^{-at}$$

と、なることが知られています。

しかるに、[0～t]分内の待ち時間の出現確率は、

$$\int_0^t f(t)\,dt=\int_0^t ae^{-at}\,dt=1-e^{-at} \quad \cdots(1)$$

ここで x＝出現数

a＝(単位時間あたりの出現期待値)＝x/観測時間

実際の観測における待ち時間t0～t分内の総待ち時間の個数をuとすると、

$$(x-1)(1-e^{-at})=u \quad \cdots(2)$$

この式をとくと出現数xが求まります。

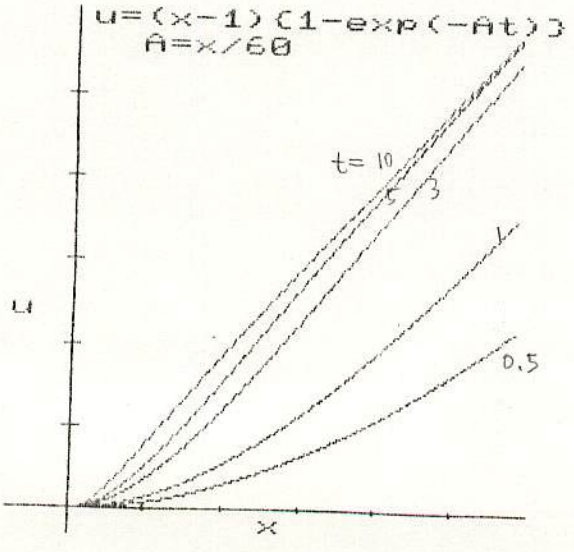

2、考察

ここでxと観則された値のちがいは何が原因であるのでしょうか。

仮りに一時間あたり2個の出現があったとします。

待ち時間(分)	xの値
1	9
2	7
3	6
4	5
10	4
15	3

左表のようになります。が、しかし今まで単にHR=2とかたずけてしまっていたものが、仮にxを真の出現と考えるならば待ち時間に着目してみるとこのようになってしまいます。

しかしながら、待ち時間1分の時に残り8個は見落しだと考えるのは、非常に不自然なのではないでしょうか？ここで初めてxの値はその観測時間内における出現期待値と考えるのです。身近なものに例をとるならば60本につき10本のあたりくじがあるくじを60本引いたが、2本しかあたらなかったと同じに考えるのです。この様に考えるならばxは、観測値や真の出現数より多くとも少なくともかまわないはずです。

3. 結論

今までは、単に真の出現数を求めるのに固執しすぎたのではないでしょうか、空間の個数密度が、低ければ低い程真の出現のばらつきが大きくなるのは、あきらかです。この例の様な低密度の流星群の密度(個数)を求めるにあたっては、この上記の様に流星の待ち時間に着目してみるというのは、一つの有効な手段になると思われます。

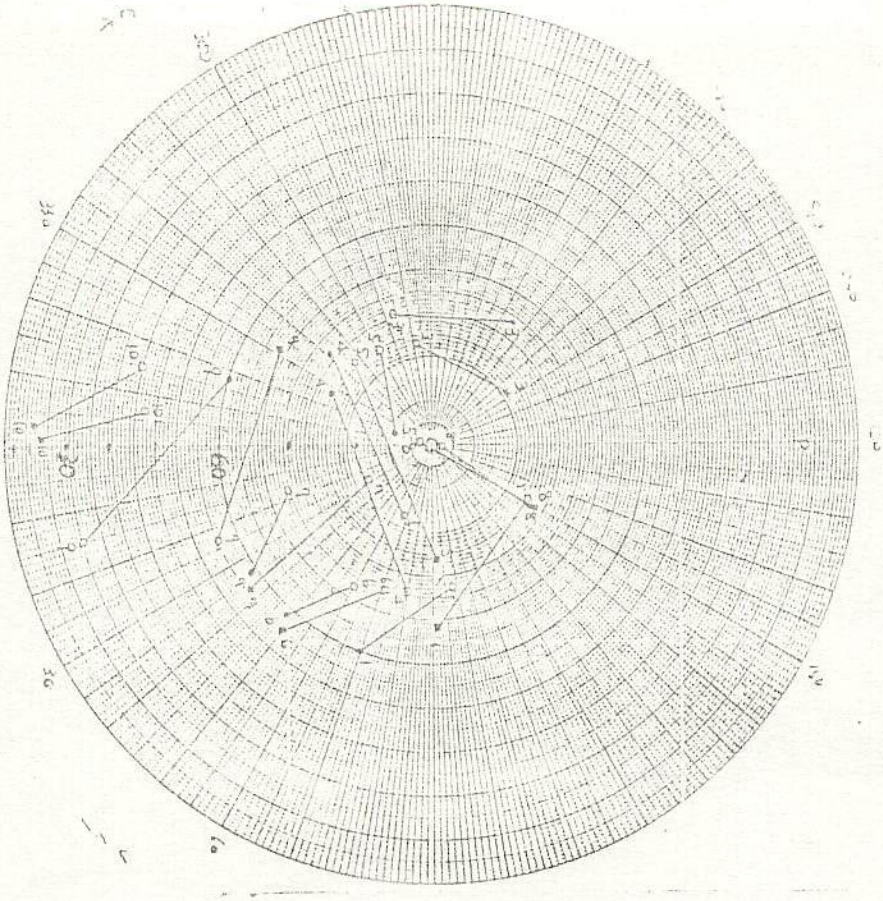

A.エネ

図1. プロット流星と放射点の位置との比較（東京）

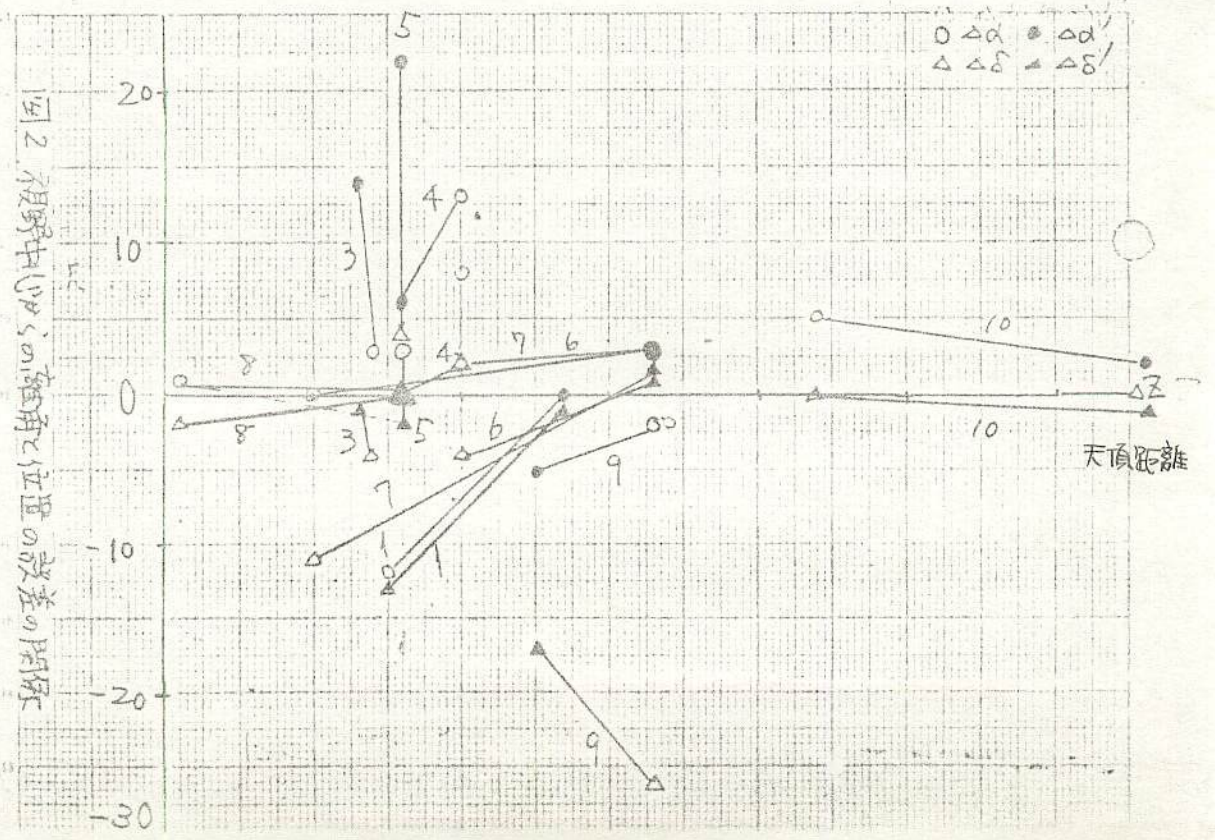

図2. 放射点からの距離と天頂距離との関係

MSS-023

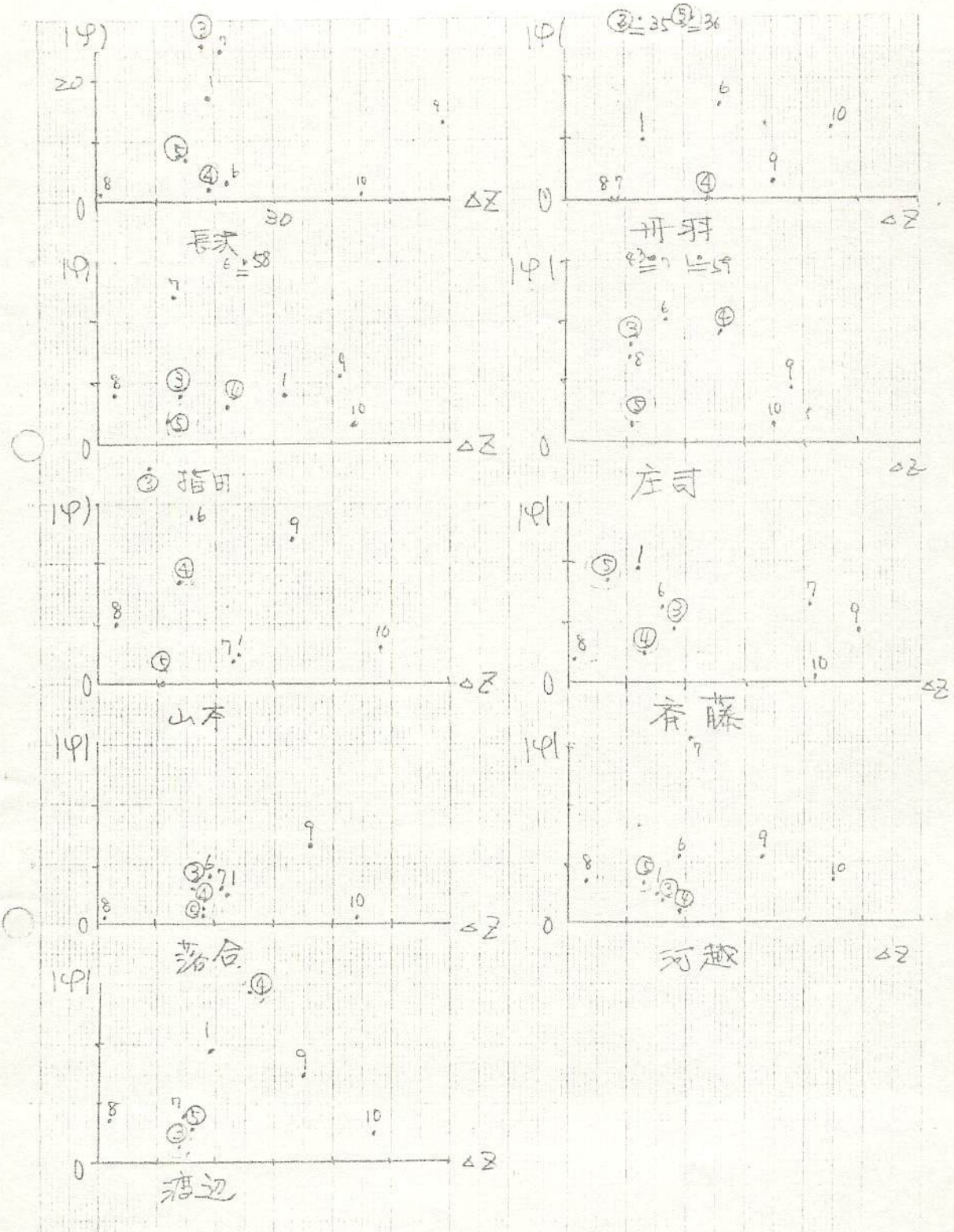

図3、視野中心からの離心と方向誤差の関係

Vol. 34 (1983), No. 2

DEPENDENCE OF THE OBSERVED RATE OF METEORS ON THE ZENITH DISTANCE OF THE RADIANT

J. Zvolánková

Astronomical Institute, Slovak Academy of Sciences, Dúbravská cesta, 842 28 Bratislava, Czechoslovakia

Received 21 January 1982

ЗАВИСИМОСТЬ НАБЛЮДАЕМОЙ ЧАСТОТЫ МЕТЕОРОВ ОТ ЗЕНИТНОГО РАССТОЯНИЯ РАДИАНТА

На основании свыше 17 000 наблюдений Персеид невооруженным глазом полученных в обсерватории Скальнате Плесо в течение 9 лет, определен показатель степени γ поправочного фактора $\cos^{\gamma} z$ для перевода наблюдаемой частоты метеоров при зенитном расстоянии радианта z на частоту для радианта в зените. Полученная величина показателя степени $\gamma = 1.47 \pm 0{,}11$ очень близка к средней величине применяемых крайних значений $\gamma = 1$ и $\gamma = 2$.

Using more than 17 000 visual records of the Perseids made at the Skalnaté Pleso Observatory over a period of 9 years, the exponent γ in the reduction factor $\cos^{\gamma} z$ was derived for reducing the rate of meteors observed at zenith distance of the radiant z to the rate when the radiant is in the zenith. The value of the exponent thus obtained, $\gamma = 1{\cdot}47 \pm 0{\cdot}11$, is very close to the average of the extremes used, $\gamma = 1$ and $\gamma = 2$.

1. Introduction

Meteor streams are the most suitable objects for studying the origin and dynamical evolution of interplanetary particles. Their basic structural and evolutionary characteristic is the particle density distribution in space. It is determined from the variation of the meteor rate along the trajectory along which the Earth passes through the meteor stream; the annual repetition of the Earth's passages through the same locations enables us to determine the changes along the stream orbit.

For investigating the density variation, classical visual methods of observation are still most important for several reasons. As compared to photographic observations, their statistical significance is much higher: one group of visual observers is capable of recording a much larger number of meteors in one return of the shower than the total number of photographic records now available the world over. As opposed to radar observations, mostly directional and limited by the condition of perpendicular reflection of signals, the advantages are much simpler selection effects and easier distinguishing between shower meteors and the sporadic background. An important advantage is also that only for visual observations, series of data covering many decades or even centuries are available. Moreover, visual observations are the simplest and easiest to reproduce.

2. Conditions of Visual Observation

The density variation within the meteor shower is reflected in the time variations of the meteor rate during the period of passage of the Earth through the shower. The absolute calibration of the observed rates depends on a number of factors, among which the geocentric velocity of the shower is of primary importance. Since the geocentric velocities of all the members of every meteor shower are approximately the same, the data on the relative variation of the spatial density can also be obtained without taking the calibration factors into account. They are represented in the form of an ideal rate curve as if determined by an observer under constant ideal conditions: with the observed layer of the atmosphere perpendicular to the motion of the meteors and with a perfectly clear and dark background of the sky. These ideal conditions would only occur in a fictitious case when the geocentric radiant of the meteor shower would be at one of the two poles of the sky, the observer at the appropriate pole of the Earth, the Sun close to the opposite tropic, the Moon close to new moon and the weather completely cloudless. The actual conditions differ substantially from the ideal

ones and, therefore, the observer is only capable of recording a part of the information as schematically shown in Fig. 1. The upper continuous curve in the figure represents the idealized rate variation which would be observed under the four ideal conditions mentioned above.

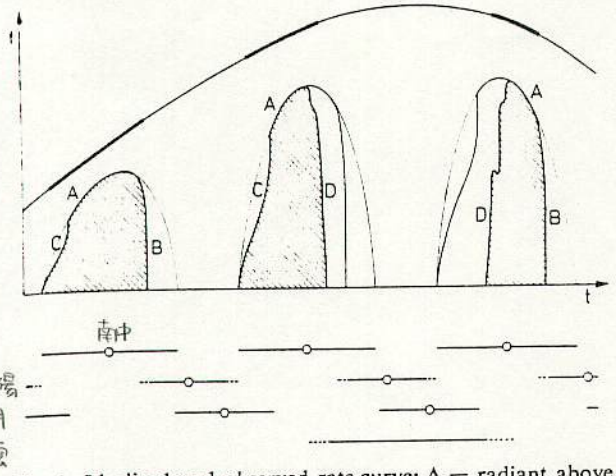

Fig. 1. Idealized and observed rate curve; A = radiant above the horizon, ◦ culmination, B = sunlight, C = moonlight, D = cloudiness (— — partial). The following intervals are indicated at the bottom of the figure: (A) in which the radiant is above the horizon, (B) in which the Sun is above the horizon (dashed line — twilight), (C) in which the Moon is above the horizon, (D) in which cloudiness occurred (dashed line — partial cloudiness).

(A) At any position outside the celestial pole, the radiant is subject to the apparent motion of the sky, reflecting the Earth's rotation. While it is below the horizon, the shower is not observed; after the rise of the radiant, the efficiency of the observation increases to the point at which it culminates, decreasing again to zero when the radiant sets. The maximum efficiency is given by the zenith distance of the radiant at its culmination and it is only 100 per cent if the radiant declination is equal to the geographic latitude of the observer, i.e. if the radiant passes through the zenith. The resultant curve represents the part of the activity which is available to radio observations, independent of the optical condition of the sky.

(B) The first limiting factor is sunshine. This makes observations impossible while the Sun is above the horizon or just below it, and continuously decreases their efficiency in time when the angular depression of the Sun reaches 15° to 5°. From a given point the daytime part of the curve cannot thus be determined and the twilight part can only be used after normalization, taking into account the brightness of the sky background.

(C) The second limiting factor is moonshine, effective the whole time the Moon is above the horizon (about 50% of the time), its intensity depending on the Moon's phase and position. When the phase is small, its effect can be neglected, the more so as it only affects observations at dusk and dawn, or just before and after. Close to full moon, the Moon has a disturbing effect nearly throughout the whole night and the decrease in the observed rate substantially diminishes its statistical weight even if the appropriate correction factors are applied.

(D) The third limiting factor is cloudiness which may either prevent observations altogether, or decrease the observed rate. The latter effect is difficult to express quantitatively, because it may be manifest in three different ways: (1) obstruction of a part of the field of view by compact cloudiness, (2) decrease of the intensity of meteor light under partly translucent cloud veil, and (3) intensifying effects (B) and (C) by scattering twilight or moonshine under semitranslucent cloudiness.

Effects (B)–(D) can be expressed satisfactorily by two quantitative parameters: by a change of the limiting magnitude of the observed meteors (equivalent to the change of the limiting magnitude of the background stars) and by diminishing the field of view. In the former case the distribution of meteors by magnitude enters the calculations, in the latter the distribution of the meteors by angular length and the manner in which the field of view is deformed. The reliability and statistical weight of the result naturally decrease with increasing correction factors.

As can be seen from Fig. 1, only the small and strongly deformed parts, marked by hatching, are available for reconstructing the whole activity curve. The calculations will only yield the sections of the upper curve, depicted as the bold line, between which the rate variation (or the relative spatial density) has to be interpolated. These sections can be filled in by means of observations from different stations; if the stations are located at different geographic longitudes, the main limiting factors (A) and (B) are phase shifted. We are thus able to fill in the gaps, which are inevitable in the data from a single station, even without interpolation. A large phase shift requires stations distributed in different continents, and this in turn requires taking into account the systematic differences in methods, conditions and results of observations (Štohl and Millman, 1973; Lindblad and Štohl, 1977).

The purpose of this paper is to derive precise methods of rectifying the rate curves, i.e. of changing from the hatched areas to the upper curve in Fig. 1. The main attention will be devoted to the dominant effect (A), i.e. to the dependence of the observed rate

on the zenith distance of the radiant, which also has important implications for the physical theory of meteors. Effect (C), i.e. the disturbing effect of the Moon, will only be considered for a particular case. The author deals with effect (B), i.e. with the reducing of observations at dusk and dawn, elsewhere (Slančíková, 1975). As regards effect (D), one can hardly expect any methodical progress because of the wide range of cloudiness forms. Besides the case with little cloudiness is rare and if cloudiness is large, no observations are made, as a rule.

3. Reduction of the Rate to the Zenith Radiant

Denoting by v the meteor flux density, referred to the plane perpendicular to the flux, v' the meteor flux density referred to any oriented plane of the horizon,

$$v' = v \cos z \,, \tag{1}$$

where z is the zenith distance of the apparent radiant.

The actual conditions of meteor observations differ slightly from this geometric model. As a result of the curvature of the Earth, we do not observe meteors in a planar layer, but in a slightly curved meniscus, bounded by concentric spherical caps. Provided that the zenith distance of the radiant is not too large, the curvature will only be reflected in an apparent decrease of altitude of the meteors low above the horizon, where the observations are not particularly efficient. However, once the zenith distance is close to 90°, the boundary of the target area is no longer a horizontal circle, but the oblique projection of the meniscus. For this case Kresák (1954) derived the relation

$$v' = \tfrac{1}{2} v\left[(2rH + H^2)^{1/2} \cos z + \right. \\ \left. + r(1 - \sin z) + H\right](2rH + H^2)^{1/2} \,, \tag{2}$$

where z is the zenith distance of the radiant, $r + H$ the radius of curvature and H the mean height of the meniscus, with r being the Earth's radius and H the altitude of the layer above the Earth's surface, in which the meteors appear.

If the altitude of the meteor layer $H = 100$ km, Eq. (2) holds true for $z \geqq 80°$.

However, much more important is the fact that the gradient of atmospheric density along the path of the meteor varies with the zenith distance of the radiant. In this way the meteoroids thus enter different regimes of interaction with the atmosphere and radiation. The existing physical theories of meteors do not give a unique answer to the question how this will change the visibility conditions of the meteor, under simultaneous decrease of maximum brightness and increase of the length of the luminous path with the zenith distance of the radiant. The cosine formula (1), which is currently used, only takes into account geometric projection and assumes that the apparent brightness of the meteor does not depend on the angle under which it enters the atmosphere. The other extreme is the dependence on $\cos^2 z$, which corresponds to the case in which the brightness varies proportionally to $\cos z$. Öpik (1940) combined both extremes as follows:

$$v' = v \cos^{\gamma} z = v\left[B \cos z + (1 - B)\cos^2 z\right]. \tag{3}$$

If $\gamma = 1$, $B = 1$, if $\gamma = 2$, $B = 0$, and if $B = 0{\cdot}5$, we obtain

$$v' = \tfrac{1}{2} v(\cos z + \cos^2 z) \,. \tag{4}$$

From the preliminary processing of the Arizona Expedition material, Öpik obtained $\gamma = 1{\cdot}34$. Later, after a detailed processing of the data, he arrived at the result $B = 1$, $\gamma = 1$ (Öpik, 1958), i.e. at a simple cosine formula for the observed meteor rate. This rather unexpected result indicates that the brightness or average rate of evaporation of meteoric matter does not depend on the angle under which the meteor enters the atmosphere. This cannot be explained by the original theory of meteoric structure which considered all meteors, regardless of their size, to be compact stone or metal bodies. However, it agrees quite well with the theory which considers meteors to be dustballs (Öpik, 1954), loose assemblages of dust particles. Here shattering and atomization due to aerodynamic pressure is the primary process of ablation of a meteoroid and evaporation is a secondary process, which takes place from the small fragments or dust particles into which the meteoroid disintegrates.

In addition to these most important results, for completeness we should mention two more which concern this problem.

By processing the data collected from many years of observing the Perseids, Schiaparelli (1871) came to the conclusion that

$$v' = v \cos^{1.6} z \,. \tag{5}$$

Prentice (1953) suggested the formula

$$v' = v \cos (z - 6°) \,, \tag{6}$$

which is, of course, based on very simplified geometric considerations and does not take into account the dependence on the length of the meteor path or the intensity of light on z.

4. Processing of the Observations

The meteor shower which would conform optimally to all the conditions for application to our problem, must satisfy three conditions:

1) Its rate must be high enough to be clearly distinguishable from the rate of the sporadic background;

2) A high and not too variable level of activity must last for several rotations of the Earth, to allow the dependence on the position of the radiant to be distinguished well from the actual changes of the shower density;

3) The observable range of zenith distances of the radiant must be as large as possible to render the variations of the rate with radiant position sufficiently distinctive.

For practical purposes, condition (2) means that we have to restrict ourselves to annual regular showers. In this case the most suitable are the Perseids and Geminids. The Perseids were chosen for further treatment. At the time of their activity in July and August, the weather in Europe is more favourable and particularly much more stable then for the December Geminids. In the extensive files of observations of the Skalnaté Pleso Observatory there is not a single case of a continuous series of Geminid observations for more than 4 consecutive nights; the total number of nights in which more than 100 meteors were observed, is 7. On the other hand, for the Perseids there are 36 nights on which more than 100 meteors were observed and the observation series between 20th July and 21st August 1946 alone contains 9 such nights. On the whole, the usable material contains 33 062 records of meteors of which 17 229 are Perseid records.

The fact that only the Perseids and Geminids are suitable for determining the relations between rate and relative meteor density in the Northern Hemisphere does not, of course, mean that these relations can only be applied to these showers. On the contrary, the purpose of this study is to derive relations which can be applied universally to all showers. Corrections for the twilight effects (Slančíková, 1975) enabled us to process the unique observations of the Draconid meteor shower (Kresák and Slančíková, 1975). Similarly, one can expect the corrections for the zenith distance of the radiant to serve not only for homogeneizing many standard observations, but as an important tool in the case of rare events observed when the position of the radiant is low.

In the present paper, we processed the visual observations of the Perseid meteor shower from the years 1944–1953, with the exception of 1945, obtained at the Skalnaté Pleso Observatory. Of the total number of 17 229 observed Perseids for this period, 10 359 were selected for further treatment. All observations during which the cloudiness amounted to more than 30%, the observations disturbed by moonlight (with the exception of 1946) and all the observations of inexperienced and casual observers were discarded. The observations were divided into 444 half-hour intervals. The number of observed Perseids N_p, the net observable time t_p and the average cloudiness were determined for every observer in each interval. The solar depression was calculated for the middle of each interval at twilight. These data and the personal coefficients were used to calculate the corrected hourly rate per one observer:

$$f_o = 60\tau \sum_1^{\varepsilon} N_p \left[\sum_1^{\varepsilon} t_p / k_{op} k_{1p}\right]^{-1} \tag{7}$$

where f_o is the corrected rate, N_p the number of meteors recorded by observer p in a given interval, t_p the net time of observation in minutes, k_{op} the cloudiness coefficient after Guth (1941), k_{1p} the personal factor after Štohl (1969), ε the number of all observers who took part in the observations within a given interval, and τ is the twilight coefficient after Slančíková (1975).

In 1946, apart from the corrections mentioned, also a correction for the Moon's phase was introduced (Zvolánková, 1983). In all the other years, the observations disturbed by moonlight were omitted from further treatment.

To allow intercomparison of the rates thus obtained, the rates had to be reduced to the radiant in the zenith. The zenith rate per one observer will now be designated by f_z and the reduction factor by $\cos^{\gamma} z$. Consequently,

$$f_z = f_o / \cos^{\gamma} z \,. \tag{8}$$

The Perseids belong to the widest meteor showers with a relatively stable, annual repetition of the activity curve. Since the Earth comes very close to the orbit of the parent comet, however, the rate curve around the maximum is steep and the height of the maximum may change from year to year as evidenced by the comparison of observations from various returns (Lovell, 1954). In deriving the exponent γ from observations made in different years, it is necessary to reduce all the shower returns to a single level (Zvolánková, 1983).

5. Calculation of Exponent γ

After reducing all the shower returns to a uniform level for various exponents γ in the reduction factor

MSS-035

$\cos^{\gamma} z$, we were able to start determining the value of the exponent γ which would fit the observations best at various zenith distances of the radiant.

Rate curves were plotted for particular values of $\gamma = 1{\cdot}0$, $1{\cdot}25$, $1{\cdot}4$, $1{\cdot}5$, $2{\cdot}0$; for $\gamma = 1{\cdot}0$ the curve is in Fig. 2.

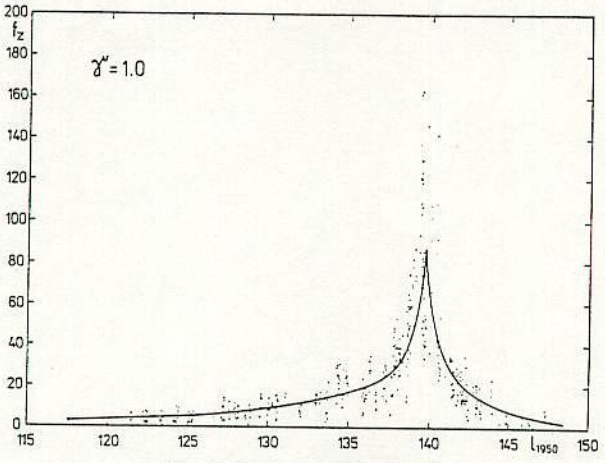

Fig. 2. Rate curve for $\gamma = 1$.

The natural logarithms of f_z were plotted in a graph; a straight line was fitted to the plotted points. The calculation was divided into two parts: before the maximum for $l_{1950} < 140°$ and after the maximum for $l_{1950} > 138°$, since the maximum activity of the Perseids shower, according to Cook (1973), falls in with $l_{1950} = 139°$. The calculation was thus made upto 140° and from 138°, in order to enable the point of intersection of the fitted lines and the time of the observed maximum of shower activity to be determined. This procedure yielded logarithmic frequency curves for all selected values of γ; the one for $\gamma = 1{\cdot}0$ is in Fig. 3.

In determining the most suitable value of exponent γ it was necessary to plot the dependence of the zenith rate on the zenith distance of the radiant.

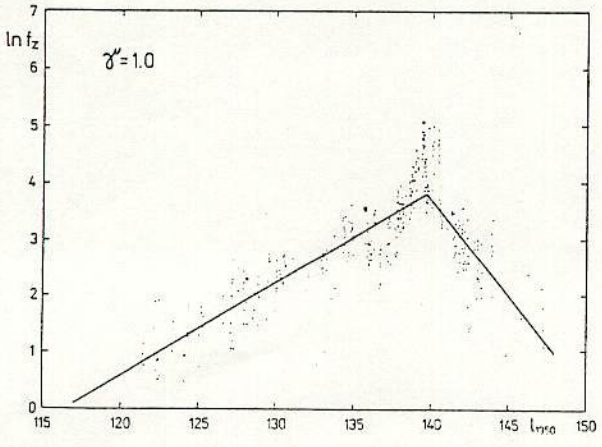

Fig. 3. Logarithmic rate curve for $\gamma = 1$.

直線近似して、＼を補正して
—— 同じ割合に直して、Fig 3~4を作った

Since the observations were made at various phases of shower activity, all the zenith rates had to be reduced to the same phase. We adopted the formula $c = 1/f_{zc}$, where f_{zc} is the zenith rate derived from the calculated rate curve, and c are the coefficients (one for each half-hour interval) by which the observed zenith rates f_{zo} have to be multiplied to reduce them to the same phase of shower activity. In other words $f_{zot} = f_{zo}/f_{zc}$ [meteors per hour]. If we take the logarithm of the whole expression,

$$\ln f_{zot} = \ln f_{zo} - \ln f_{zc} \tag{8}$$

and the expression on the r.h.s. can be determined directly in calculating the theoretical logarithmic rate curve. The values of $\ln f_{zot}$ obtained in this manner were plotted in a graph versus the zenith distance of the radiant. A straight line was fitted to the points. The exponent γ in the reduction factor $\cos^{\gamma} z$ for which the fitted line comes closest to the x-axis, can be considered the most probable, because we adopted a transformation to render $f_{zct} = 1$. All the values $\ln f_{zct} = 0$ because they lie on the x-axis for every zenith distance of the radiant.

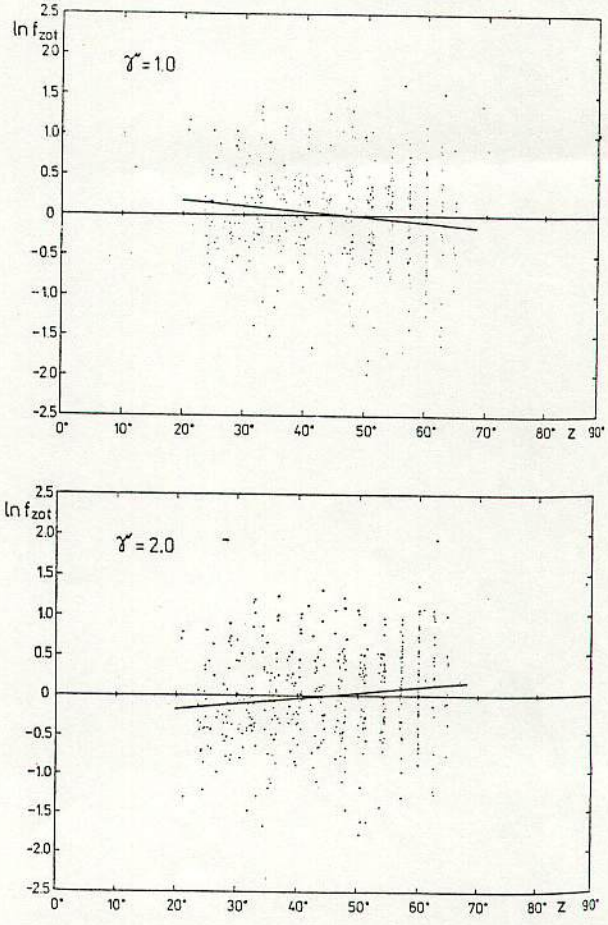

Fig. 4. Reduced logarithmic rate curves for a) $\gamma = 1$ and b) $\gamma = 2$.

Vol. 34 (1983), No. 2

Figure 4 shows $\ln f_{zot}$ plotted versus z for $\gamma = 1{\cdot}0$ and $\gamma = 2{\cdot}0$.

As one can see from the figures, the value $\gamma = 2{\cdot}0$ overestimates the rates at higher zenith distances and the value $\gamma = 1{\cdot}0$ underestimates them. Of all the exponents investigated, $\gamma = 1{\cdot}4$ is the closest to satisfying the condition $\ln f_{zct} = 0$ and it was, therefore, adopted for further treatment. The values of $\ln f_{zotc}$ for individual values of γ are in Tab. 1.

Table 1

Values of $\ln f_{zotc}$ as a function of γ

z \ γ	1·00	1·40	2·00
20°	0·1794	0·0333	−0·1734
30°	0·1120	0·0235	−0·1013
40°	0·0447	0·0138	−0·0293
50°	−0·0227	0·0040	0·0428
60°	−0·0901	−0·0058	0·1149
70°	−0·1574	−0·0155	0·1870

6. Testing the Results

In order to determine the interval in which the exponent $\gamma = 1{\cdot}4$ is valid with a certainty of 90% and 50%, the results were tested by means of Student's t-test. This test can be used to investigate the difference $b - \beta$ between the selectional regression coefficient b and the assumed value of the theoretical regression coefficient β. The t-test can be applied to random selections from (approximately) normal distributions (Lowell Wine, 1964).

The plotted curve of b-values and its limiting values versus the exponent γ indicates that, with a confidence of 90%, all exponents $\gamma\langle 1{\cdot}19;\ 1{\cdot}75\rangle$ and, with a confidence of 50%, all exponents $\gamma\langle 1{\cdot}35;\ 1{\cdot}58\rangle$ are satisfactory, the average value being $\gamma = 1{\cdot}47$ as shown in Fig. 5.

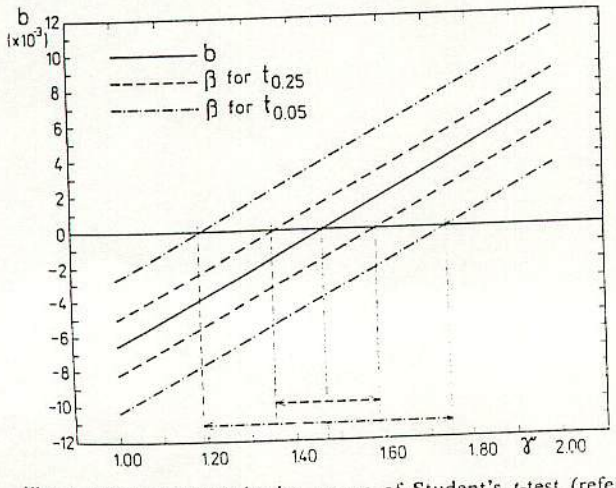

Fig. 5. Testing of results by means of Student's t-test (refer to text).

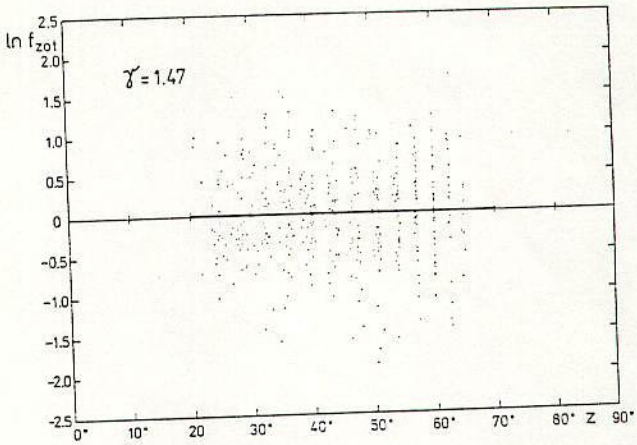

Fig. 6. Reduced logarithmic rate curve for $\gamma = 1{\cdot}47$.

Figure 6 shows $\ln f_{zot}$ plotted versus z for $\gamma = 1{\cdot}47$ for comparison with Fig. 4.

The values of the reduction factors $\cos^{\gamma} z$ for various values of γ and various zenith distance of the radiant z are given in Tab. 2.

Table 2

Values of zenith reduction factors

z	$\cos^{\gamma} z$ for γ				
	1·00	1·35	1·47	1·58	2·00
0°	1·00	1·00	1·00	1·00	1·00
10°	0·98	0·98	0·98	0·98	0·97
20°	0·94	0·92	0·91	0·91	0·88
30°	0·87	0·82	0·81	0·80	0·75
40°	0·77	0·70	0·68	0·66	0·59
50°	0·64	0·55	0·52	0·50	0·41
60°	0·50	0·39	0·36	0·33	0·25
70°	0·34	0·24	0·21	0·18	0·12
80°	0·17	0·09	0·08	0·06	0·03

With regard to the quality and quantity of the observational material used and to the selection of the shower, one may hardly expect to determine the exponent γ with a considerably higher accuracy in future. The final result

$$\gamma = 1{\cdot}47 \pm 0{\cdot}11 \text{ (p.e.)}$$

is very close to the average of the extremes used, $\gamma = 1$ and $\gamma = 2$. We may certainly claim that the nearly generally used geometric concept, assuming $\gamma = 1$, is not satisfactory for accurate treatment. On this concept are sometimes based studies dealing

MSS-035

with the distribution of sporadic radiants in the sky and systematic errors are then introduced into the results. Similarly, errors are incurred in the rate curves of meteor showers, particularly if the curves are based on shorter observations made from different locations during one night, and in comparing the activity of different showers. In this case the activity of showers with an unfavourable (low) position of the radiant is underestimated as compared with the activity of showers which can be observed well. An example is the pair of showers belonging to the meteor stream of Comet Halley, the η Aquarids and Orionids. Many references give a higher reduced rate for the Orionids, although in their period the Earth is substantially more remote from the orbit of the parent comet. This discrepancy can be explained at least partly by the use of the incorrect value of $\gamma = 1$, which decreases the rate of the η Aquarids substantially. A cofactor is the frequent neglection of the increase in the brightness of the sky, because the radiant of the η Aquarids rises just before dawn.

The results of this study promise substantially higher accuracy in dealing with all meteor showers, in deriving the actual variations of the spatial density in various streams and in comparing them, in combining observations from different places and in processing important observations made under geometrically unfavourable conditions.

Acknowledgements

The author would like to thank Dr. L. Kresák and Dr. J. Štohl for valuable advice and comments.

REFERENCES

Cook, A. F.: 1973, in Evolutionary and Physical Properties of Meteoroids (NASA SP-319, Washington, DC), p. 203
Guth, V.: 1941, Mitt. u. Beob. d. Tschech. Astron. Ges. 6, 9.
Kresák, L.: 1954, Bull. Astron. Inst. Czechosl. 6, 120.
Kresák, L.; Slančíková, J.: 1975, Bull. Astron. Inst. Czechosl. 26, 327.
Lindblad, B. A.; Štohl, J.: 1977, Bull. Astron. Inst. Czechosl. 28, 321.
Lovell, A. C. B.: 1954, Meteor Astronomy (University Press, Oxford).
Lowell Wine, R.: 1964, Statistics for Scientists and Engineers (Prentice-Hall, Inc., Englewood Cliffs, N. J.)
Öpik, E. J.: 1940, Tartu Obs. Publ. 30, 33.
—*:* 1954, Armagh Obs. Contr. 14, 13.
—*:* 1958, Armagh Obs. Contr. 26, 47.
Prentice, J. P. M.: 1953, J. Brit. Astron. Assoc. 63, 176.
Schiaparelli, J. V.: 1871, Entwurf einer astronomischen Theorie der Sternschnuppen (Stettin).
Slančíková, J.: 1975, Bull. Astron. Inst. Czechosl. 26, 321.
Štohl, J.: 1969, Contr. Astron. Obs. Skalnaté Pleso 4, 25.
Štohl, J.; Millman, P. M.: 1973, Bull. Astron. Inst. Czechosl. 24, 321.
Zvolánková, J.: 1983, in preparation.